

## An experimental investigation of the angular dependence of diffusion-driven flow

Thomas Peacock<sup>a)</sup>

*Department of Mechanical Engineering, Massachusetts Institute of Technology, Cambridge, Massachusetts 02139*

Roman Stocker and Jeff M. Aristoff

*Department of Mathematics, Massachusetts Institute of Technology, Cambridge, Massachusetts 02139*

(Received 25 March 2004; accepted 15 April 2004; published online 6 August 2004)

We present experimental results on diffusion-driven flow along an inclined wall in a stably stratified fluid. The experiments focus on the dependence of the velocity in the buoyancy layer on the angle of inclination. The increase of velocity with decreasing angle is in agreement with theory for larger angles. For small angles, where current theory breaks down, the velocity tends to zero and an angle of maximum velocity exists. © 2004 American Institute of Physics. [DOI: 10.1063/1.1763091]

Convection in a stably stratified fluid, generated through the combined action of diffusion and gravity, was first identified by Phillips<sup>1</sup> and Wunsch.<sup>2</sup> The phenomenon occurs at an inclined boundary across which there is a discontinuity in diffusivity, as shown in Fig. 1. The necessity of flux continuity across the boundary gives rise to a thin buoyancy layer adjacent to the wall, in which otherwise horizontal isopycnals adjust to meet the wall at an angle. Fluid within this thin layer is buoyant with respect to the bulk, generating convection that develops to a steady state in which viscous and buoyancy forces balance. The net convective flux associated with this flow is upslope if the inclined wall bounds the fluid from below, as shown in Fig. 1, and downslope if the fluid is bound from above. For salt-stratified fluids the characteristic flow velocity is of the order of centimeters per hour; such flows have applications in geophysical systems where the timescale is large (e.g., flow in a fissure), and may be applicable to transport in microchannels, where the lengthscale is small. For liquid metals, the effect is potentially strong enough to induce turbulence.<sup>1</sup>

Phillips<sup>1</sup> and Wunsch<sup>2</sup> independently and simultaneously obtained an analytical solution for unidirectional diffusion-driven flow along an inclined wall. Their theory predicts that the velocity along the inclined wall,  $u$ , as a function of the normal coordinate,  $\eta$ , is

$$u(\eta) = 2\kappa\gamma \cot\alpha e^{-\gamma\eta} \sin\gamma\eta, \quad (1)$$

where

$$\gamma^{-1} = \left( \frac{N^2 \sin^2\alpha}{4\nu\kappa} \right)^{-1/4} \quad (2)$$

is the characteristic buoyancy layer thickness,  $\kappa$  is the molecular diffusion coefficient,  $\nu$  is the kinematic viscosity,  $\alpha$  is the angle the wall makes with the horizontal,  $N = [-g/\rho_0(\partial\rho/\partial z)]^{1/2}$  is the buoyancy frequency,  $g$  is the acceleration of gravity,  $\rho$  is the density,  $\rho_0$  is the average den-

sity, and  $z$  is the vertical coordinate (positive upwards). Aside from the prefactor  $\cot\alpha$  the solution is the same as that obtained by Prandtl<sup>3</sup> for buoyancy driven convection up a heated inclined sidewall.

The form of the velocity profile (1) is shown in Fig. 1. The profile contains a weak reverse flow that contributes less than 5% to the volume flux

$$Q = \int_0^\infty u d\eta = \kappa \cot\alpha. \quad (3)$$

This flux is only a function of the diffusivity and the slope of the inclined wall, and is independent of the stratification. The mean velocity associated with the flow is therefore

$$\bar{u} \sim Q/\gamma = \kappa\gamma \cot\alpha. \quad (4)$$

This is approximately half the maximum velocity  $u_{\max} = \sqrt{2}e^{-\pi/4}\kappa\gamma \cot\alpha$ , which occurs at  $\gamma\eta = \pi/4$ .

The solution (1) is singular in the limit  $\alpha \rightarrow 0$ . Wunsch<sup>2</sup> showed that the solution breaks down when

$$\sin\alpha < O(R^{-1/4}), \quad (5)$$

where

$$R = \frac{N^2 L^4}{\nu\kappa} \quad (6)$$

is a Rayleigh number and  $L$  is the scale height of the stratification. For smaller angles, the approach of Wunsch illustrates that buoyancy forces perpendicular to the inclined wall cannot be ignored, which is incompatible with unidirectional flow.

On physical grounds, flow induced in the buoyancy layer must vanish as  $\alpha \rightarrow 0$ , which corresponds to the limit of a horizontal boundary. One must therefore conclude that an angle  $\alpha_{\max}$  exists at which properties of diffusion-driven flow along an inclined wall, such as velocity or volume and mass transport, are maximized. Further theoretical and numerical work on this problem has been performed<sup>4-10</sup> but there are no explicit results for the angular dependence of diffusion-

<sup>a)</sup>Electronic mail: tomp@mit.edu

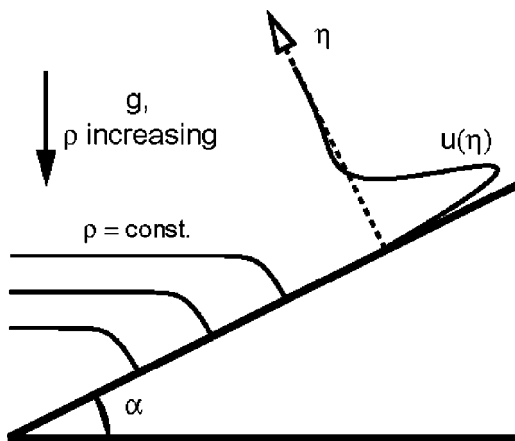


FIG. 1. Schematic of upslope diffusion-driven flow. The velocity profile  $u(\eta)$  is shown.

driven flow in the small angle limit. Furthermore, aside from the demonstration of Phillips,<sup>1</sup> there have been few experimental investigations of diffusion-driven flow. Qualitative visualizations were performed by Chashechkin and co-authors,<sup>11–13</sup> who used Schlieren techniques to visualize stratified flow past a cylinder. The only quantitative experimental study was performed by Luna *et al.*,<sup>14</sup> who visualized flow in a fissure at  $45^\circ$  using particle tracking methods. Interestingly, there is no singularity at  $\alpha=0^\circ$  in the unidirectional solution for this problem; rather, flow quantities are maximized at  $45^\circ$ .<sup>1</sup>

Our experiments were performed in a Plexiglas tank (40 cm  $\times$  25 cm  $\times$  2.5 cm) with a sloping Plexiglas surface inclined at angle  $\alpha$ , ranging from  $0.6^\circ$  to  $75.0^\circ$ . The angle of inclination was measured from a digital image of the sloping wall and a plumb line to an accuracy of  $0.1^\circ$ . A linear stratification was achieved by filling the tank with salt water from below using a double bucket system. The average buoyancy frequency for the experiments was  $N = 2.11 \pm 0.11 \text{ s}^{-1}$ ; the quantity  $N^{1/2}$ , which arises in expression (2) for  $\gamma$ , therefore varied by less than 3%. A small amount of Blue Dextran dye was carefully injected into a reservoir at the base of the inclined wall. Blue Dextran was chosen because its high molecular weight ( $\sim 40\,000$ ) gives it a much lower diffusivity in water than salt, allowing it to follow the flow almost without diffusing. The density of the dye mixture was slightly greater ( $\sim +5 \text{ kg/m}^3$ ) than that of the ambient fluid at the depth of injection, allowing the dye to settle in the reservoir.

Dye from the reservoir was drawn up by the diffusion-driven flow and transported along the wall. A sequence of three images portraying the advancing dye front for  $\alpha=3.6^\circ$  is shown in Fig. 2. The pictures were taken using a digital camera with a resolution of 15 pixels/mm, and have been stretched by a factor of 3 in the vertical for improved visualization. The camera was inclined at a small angle to the horizontal, so that the buoyancy layer was not viewed directly from the side, but from slightly above. From this perspective it was easier to visualize the buoyancy layer because of its apparent increased thickness. In agreement with theory,<sup>1,2</sup> the characteristic thickness of the buoyancy layer

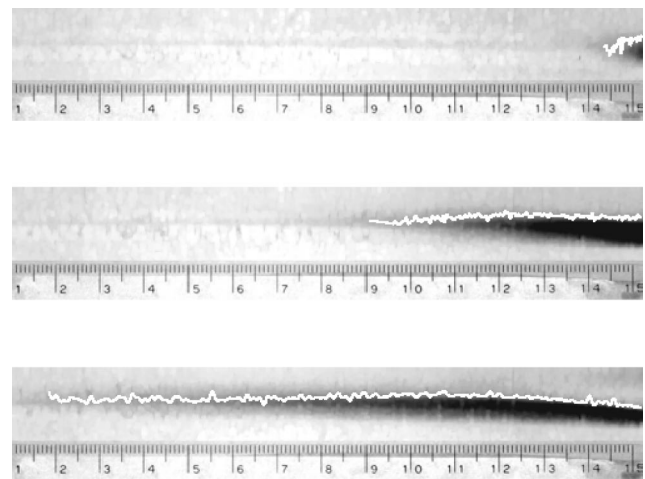


FIG. 2. Three snapshots of the advancing dye front for  $\alpha=3.6^\circ$ . The reservoir of dye is located to the right of the images, and the black dye front can be seen advancing from right to left. The images were rotated by  $-\alpha$  to facilitate processing. From top to bottom the three images correspond to times 10, 100, and 200 min after the start of the experiment. The units on the ruler are centimeters. Superimposed in white on each image is the dye interface, reconstructed using the image processing methods.

was of the order of 1 mm and noticeably increased with decreasing angle.

Typically an image was recorded every 5 min. Each image was saved in red–green–blue (RGB) format, with the dye showing up most strongly in the blue field. To determine the position of the dye front as a function of time the first image was subtracted from all subsequent images. The position of the front was then defined to be the furthest pixel along the wall for which the blue value exceeded a minimum threshold (20 out of 255). This threshold was the smallest value that allowed for detection of the motion of the dye front above the background noise level. Choosing a higher threshold value did not noticeably affect the measured velocity.

Figure 3 shows the data obtained for the position of the

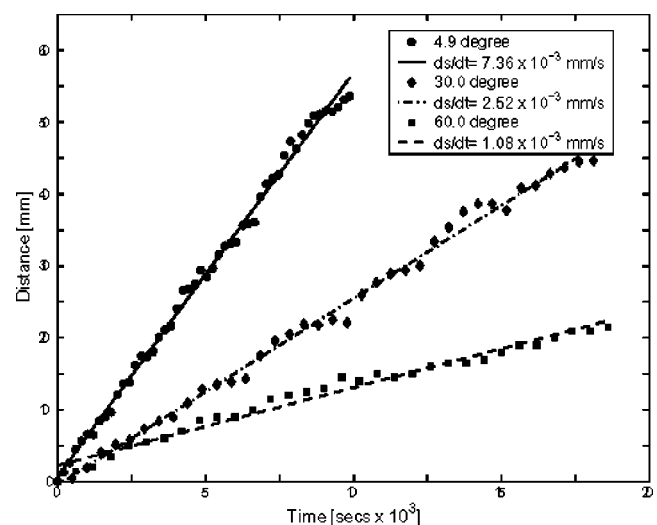


FIG. 3. Distance traveled by the dye front vs time for three experiments. A straight line has been fitted to each set of data, showing that a constant speed is attained.

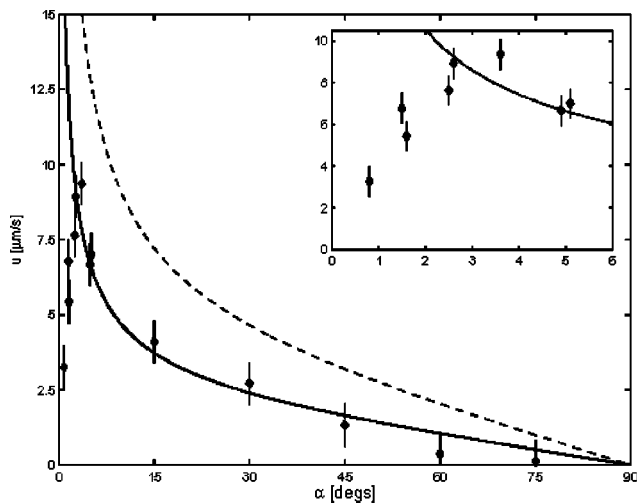


FIG. 4. Plot of the experimental velocity measurements as a function of the angle of inclination. Each diamond corresponds to one experiment. The solid line is the theoretical mean velocity  $\bar{u}$  and the dashed line is the theoretical maximum velocity  $u_{\max}$ . The error bars denote the estimated experimental uncertainty. The inset shows the small angle data in more detail.

front as a function of time, for angles  $4.9^\circ$ ,  $30.0^\circ$ , and  $60.0^\circ$ . The speed of the front was determined from a least-squares linear fit to the data. A constant slope is evident in each case, indicating that a steady state was reached by the flow. The results of the least-squares fit are presented in Fig. 4, in which the measured speed is plotted as a function of the angle of inclination. Also presented are the two theoretical curves for the maximum velocity  $u_{\max}$  and the mean velocity  $\bar{u}$ . The angular dependence of the data agrees remarkably well with theory for angles larger than  $5^\circ$ . As one might anticipate, the measured velocity is closer to  $\bar{u}$  than  $u_{\max}$ , as the experiment was not designed to accurately resolve the velocity profile within the buoyancy layer.

For angles smaller than  $5^\circ$ , the results in Fig. 4 diverge from the theoretical solution (1), as anticipated. The inset of Fig. 4 highlights the angular dependence of the measured speed at small angles, showing that it tends to zero with the inclination of the wall. The angle of maximum velocity can therefore be determined to be  $\alpha_{\max} = 2.8^\circ \pm 1.0^\circ$ . For comparison, Wunsch<sup>2</sup> predicts that the theoretical solution (1) breaks down at the angle given by Eq. (5), which for our experiments is in the range  $0.03^\circ < \alpha < 0.3^\circ$ ; in calculating the lower and upper limits of this range we have used the length

and width of the inclined wall, respectively, as our value for  $L$ .

In conclusion, we have presented the first experimental validation of the angular dependence of the Phillips–Wunsch diffusion-driven flow. Quantitative agreement between the measured velocity of a dye front and the mean theoretical velocity in the buoyancy layer is very good. The dependence of the velocity on the angle of the sloping wall is in accord with theoretical predictions for larger angles. For our experiment we deduce that the angle of maximum velocity for water stratified by salt is  $\alpha_{\max} = 2.8^\circ \pm 1.0^\circ$ . In general, we expect that this value will depend on the Rayleigh number  $R$  and the Prandtl number  $\nu/\kappa$ . Below  $\alpha_{\max}$  the velocity profile departs from the Phillips–Wunsch flow, as anticipated.

The authors would like to thank Neil Balmforth for useful discussions and Martha Buckley for her involvement with some of the experiments. J.M.A. was supported by the MIT UROP program.

- <sup>1</sup>O. M. Phillips, "On flows induced by diffusion in a stably stratified fluid," *Deep-Sea Res.* **17**, 435 (1970).
- <sup>2</sup>C. Wunsch, "On oceanic boundary mixing," *Deep-Sea Res.* **17**, 293 (1970).
- <sup>3</sup>L. Prandtl, *The Essentials of Fluid Dynamics* (Blackie, London, 1952), p. 452.
- <sup>4</sup>C. Quon, "Diffusively induced boundary layers in a tilted square cavity," *J. Comput. Phys.* **22**, 459 (1976).
- <sup>5</sup>P. F. Linden and J. E. Weber, "The formation of layers in a double-diffusive system with a sloping boundary," *J. Fluid Mech.* **81**, 757 (1977).
- <sup>6</sup>A. W. Woods, "Boundary-driven mixing," *J. Fluid Mech.* **226**, 625 (1991).
- <sup>7</sup>A. W. Woods and S. J. Linz, "Natural convection in a tilted fracture," *J. Fluid Mech.* **241**, 59 (1992).
- <sup>8</sup>A. V. Kistovich and Yu. D. Chashechkin, "The structure of transient boundary flow along an inclined plane in a continuously stratified medium," *J. Appl. Mech.* **57**, 633 (1993).
- <sup>9</sup>V. G. Baydulov and Yu. D. Chashechkin, "The diffusion effects on the boundary flow in a continuously stratified fluid," *Izv., Acad. Sci., USSR, Phys. Atmos. Ocean* **29**, 641 (1994).
- <sup>10</sup>E. J. Shaughnessy and J. W. Van Gilder, "Low Rayleigh number conjugate convection in straight inclined fractures in rock," *Numer. Heat Transfer, Part A* **28**, 389 (1995).
- <sup>11</sup>V. G. Baydulov and Yu. D. Chashechkin, "A boundary current induced by diffusion near a motionless horizontal cylinder in a continuously stratified fluid," *Izv., Acad. Sci., USSR, Atmos. Oceanic Phys.* **32**, 751 (1996).
- <sup>12</sup>Yu. D. Chashechkin, "Schlieren visualisation of a stratified flow around a cylinder," *J. Visualisation* **1**, 345 (1999).
- <sup>13</sup>Yu. D. Chashechkin and V. V. Mitkin, "Experimental study of a fine structure of 2D wakes and mixing past an obstacle in a continuously stratified fluid," *Dyn. Atmos. Oceans* **34**, 165 (2001).
- <sup>14</sup>E. Luna, A. Córdova, A. Medina, and F. J. Higuera, "Convection in a finite tilted fracture in a rock," *Phys. Lett. A* **300**, 449 (2002).